American Journal of Pathology, Vol. 167, No. 3, September 2005

Immunopathology and Infectious Disease

The Role of Antigenic Drive and Tumor-Infiltrating Accessory Cells in the Pathogenesis of *Helicobacter*-Induced Mucosa-Associated Lymphoid Tissue Lymphoma

Anne Mueller,* Jani O'Rourke,† Pauline Chu,‡ Amanda Chu,* Michael F. Dixon,§ Donna M. Bouley,‡ Adrian Lee,† and Stanley Falkow*

From the Departments of Microbiology and Immunology and Comparative Medicine,‡ Stanford University Medical School, Stanford, California; the School of Biotechnology and Biomolecular Sciences,† University of New South Wales, Sydney, New South Wales, Australia; and the Department of Histopathology,§ University of Leeds, Leeds, United Kingdom*

Gastric B-cell lymphoma of mucosa-associated lymphoid tissue type is closely linked to chronic *Helicobacter pylori* infection. Most clinical and histopathological features of the tumor can be reproduced by prolonged *Helicobacter* infection of BALB/c mice. In this study, we have addressed the role of antigenic stimulation in the pathogenesis of the lymphoma by experimental infection with *Helicobacter felis*, followed by antibiotic eradication therapy and subsequent re-infection. Antimicrobial therapy was successful in 75% of mice and led to complete histological but not "molecular" tumor remission. Although lympho-epithelial lesions disappeared and most gastric lymphoid aggregates resolved, transcriptional profiling revealed the long-term mucosal persistence of residual B cells. Experimental re-introduction of *Helicobacter* led to very rapid recurrence of the lymphomas, which differed from the original lesions by higher proliferative indices and more aggressive behavior. Immunophenotyping of tumor cells revealed massive infiltration of lesions by $CD4^+$ T cells, which express CD28, CD69, and interleukin-4 but not interferon-γ, suggesting that tumor B-cell proliferation was driven by Th 2-polarized, immunocompetent, and activated T cells. Tumors were also densely colonized by follicular dendritic cells, whose numbers were closely associated with and predictive of treatment outcome. ***(Am J Pathol 2005, 167:797–812)***

The bacterial pathogen *Helicobacter pylori* colonizes the gastric mucosa of roughly 50% of the world's population and triggers a strong local inflammatory response. Chronic inflammation due to persistent *H. pylori* infection can give rise to organized lymphoid follicles in the gastric mucosa. This so-called mucosa-associated lymphoid tissue (MALT) constitutes a premalignant condition that can ultimately progress to "low-grade gastric B-cell lymphoma of MALT type" in a small subset of infected individuals. The current model of MALT lymphomagenesis assumes that one or more neoplastic clones with characteristics of marginal zone B cells arise from this background of organized MALT, colonize, and displace the original follicles, and eventually destroy the gastric glands and form lympho-epithelial lesions.[1] Although MALT lymphoma is generally considered an indolent tumor because of its slow growth and low propensity for spread, a small percentage of cases undergo high-grade transformation, thereby limiting treatment options and resulting in unfavorable disease outcomes.

It is now generally accepted that the antigenic stimulation required to initiate the lympho-proliferative processes of gastric MALT lymphomagenesis is provided by *H. pylori* infection.[2–6] A number of studies showed a high prevalence of *H. pylori* infection in patients with MALT lymphoma.[7–9] In addition, retrospective serological studies demonstrated that individuals infected with this bacterium have a higher risk of developing lymphoma.[10] Most importantly, eradication of the bacterium can lead to regression of the lymphoma, especially in its early stages.[5,11,12] Therefore, defining the precise role this

Supported by National Institutes of Health grants CA92229 and AI38459 (to the laboratory of S.F.), by the Emmy-Noether-Program of the Deutsche Forschungsgemeinschaft, Germany (MU1675/1-1 to A.M.), and by National Health and Medical Research Council (Australia) grant 9936694 (to J.O.R.).

Accepted for publication June 14, 2005.

Address reprint requests to Anne Mueller, Department of Microbiology and Immunology, Stanford University Medical School, 299 Campus Dr., Stanford, CA 94305. E-mail: muellera@stanford.edu.

bacterium plays in disease initiation and progression is critical to our further understanding of the etiology of the disease.

We have previously shown that chronic experimental infection of BALB/c mice with the gastric bacterium *Helicobacter felis* results in the development of histopathological lesions that closely resemble those seen in patients diagnosed with gastric MALT lymphoma.[13] In the same model system, we were able to induce tumor regression by antimicrobial eradication therapy,[14] thereby further emphasizing the parallels between the diseases in humans and the mouse model. Interestingly, vaccination against *Helicobacter* using a whole-cell sonicate vaccine in conjunction with cholera toxin proved effective in preventing lymphoma formation in the mouse model.[15,16] More recently, we uncovered distinct transcriptional signatures that correlate with specific histopathological disease stages and allow us to accurately predict the pathology of previously unclassified samples.[17]

In the present study, we have addressed the effects of the presence and absence of antigenic stimulation by eradicating and subsequently re-introducing *H. felis* into a group of mice and comparing them with littermates that were persistently infected or had received triple therapy. We combined whole-genome gene expression profiling and detailed immunohistochemical analysis to obtain clues about the nature and proliferative propensity of B cells in progressing versus regressing tumors, the cellular composition of the tumors, and the role accessory cells play in tumor progression.

Materials and Methods

Animal Experimentation and Histological Analysis of Gastric Tissues

Specific pathogen-free female BALB/c mice were obtained from the Animal Resources Centre, Canning Vale, Western Australia, Australia at 6 weeks of age. Animals were maintained under clean conditions, and all protocols involving animal experimentation were approved by the Animal Care and Ethics Committee of the University of New South Wales. Three groups of mice were infected orally with *H. felis* (CS1, ATCC 49179) as described previously[13] and left for 18 months to allow for lymphoma development; a fourth group remained uninfected as a control. Two of the infected groups then received triple therapy (bismuth, metronidazole, and tetracycline) for 2 weeks as described previously.[18] Four weeks after the start of therapy, one of these groups was then re-infected with *H. felis.* All animals were killed 4 months after re-infection (Figure 1A). Gastric samples were collected for histological assessment and RNA extraction. One-half of each stomach was fixed in 10% buffered formalin and embedded in paraffin, and the rest was snap-frozen in liquid nitrogen for RNA preparation. Sections were stained with May-Grünwald-Giemsa for grading of bacterial colonization on a 0- to 4-point scale as described previously[19] in four different regions of the stomach (antrum, body, antrum/body, and body/cardia transitional zones). Hematoxylin and eosin (H&E)-stained sections were also graded for histopathological changes as described previously.[17] The presence of lymphoid aggregates and lympho-epithelial lesions was graded on a 0 to 3 scale, and a diagnosis of lymphoma was also noted. All slides were coded and examined blind.

RNA Extraction, Labeling, and Hybridization and Data Analysis

RNA extractions from one-half of every stomach were performed using Trizol reagent according to the manufacturer's instructions (Invitrogen Life Technologies, Carlsbad, CA). Total RNA was then further purified using RNeasy kits (Qiagen, Chatsworth, CA). Gene expression profiling with 38,000 element spotted murine cDNA microarrays was performed as described.[17] The reference for all arrays used in this study consisted of pooled cDNA extracted from stomachs of five age-matched uninfected control animals. Microarray data were stored in the Stanford Microarray Database.[20] Data were filtered with respect to spot quality (spots with regression correlations <0.6 were omitted) and data distribution (genes whose $\log_2$ of red-to-green normalized ratio is more than 1.5 SD away from the mean in at least three arrays were selected) before clustering. Only genes for which information was available for >70% of arrays were included. Data were $\log_2$ transformed and analyzed using CLUSTER and TREEVIEW.[21] Data from all of the arrays analyzed in this paper are available at http://genome-www5.stanford.edu/.

Immunohistochemistry

Sequential 4-μm paraffin sections were stained with antibodies specific for the following murine antigens: CD45R/B220 (1:100; rat clone RA3–6B2; PharMingen/BD Biosciences, San Jose, CA), IgM (1:50; polyclonal goat serum; Southern Biotech, Birmingham, AL), CD79α (1:25; rat clone HM57; Dako, Carpinteria, CA), CD3 (prediluted polyclonal rabbit serum; Biomeda, Foster City, CA), F4/80 (1:75; rat clone A3–1; Abcam Limited, Cambridge, UK), S100 (prediluted polyclonal rabbit serum; Dako, Carpinteria, CA), and proliferating cell nuclear antigen (PCNA; 1:10; mouse clone PC10; Zymed Labs Inc., South San Francisco, CA). Antigen retrieval was performed by boiling for 5 minutes in 10 mmol/L citrate buffer, pH 6, with the following exception: the detection of CD79a and IgM required heat retrieval in 10 mmol/L Tris and 1 mmol/L EDTA, pH 9, and the detection of F4/80 required trypsin digestion.

Frozen 5-μm sections were dried overnight, briefly fixed in acetone, dried for several more hours, and stained with antibodies against the following additional murine antigens: Ki67 (1:100; rat clone TEC 3; Dako, Carpinteria, CA), INF-γ (1:25; rat clone RMMG-1; Chemicon International, Temecula, CA), interleukin (IL)-4 (1:25; rat clone BVD4-1D11; Imgenex, San Diego, CA), CD4 (1:25; rat clone RM4-5; PharMingen/BD Biosciences), CD8 (1:50; rat clone KT15; Chemicon International, Te-

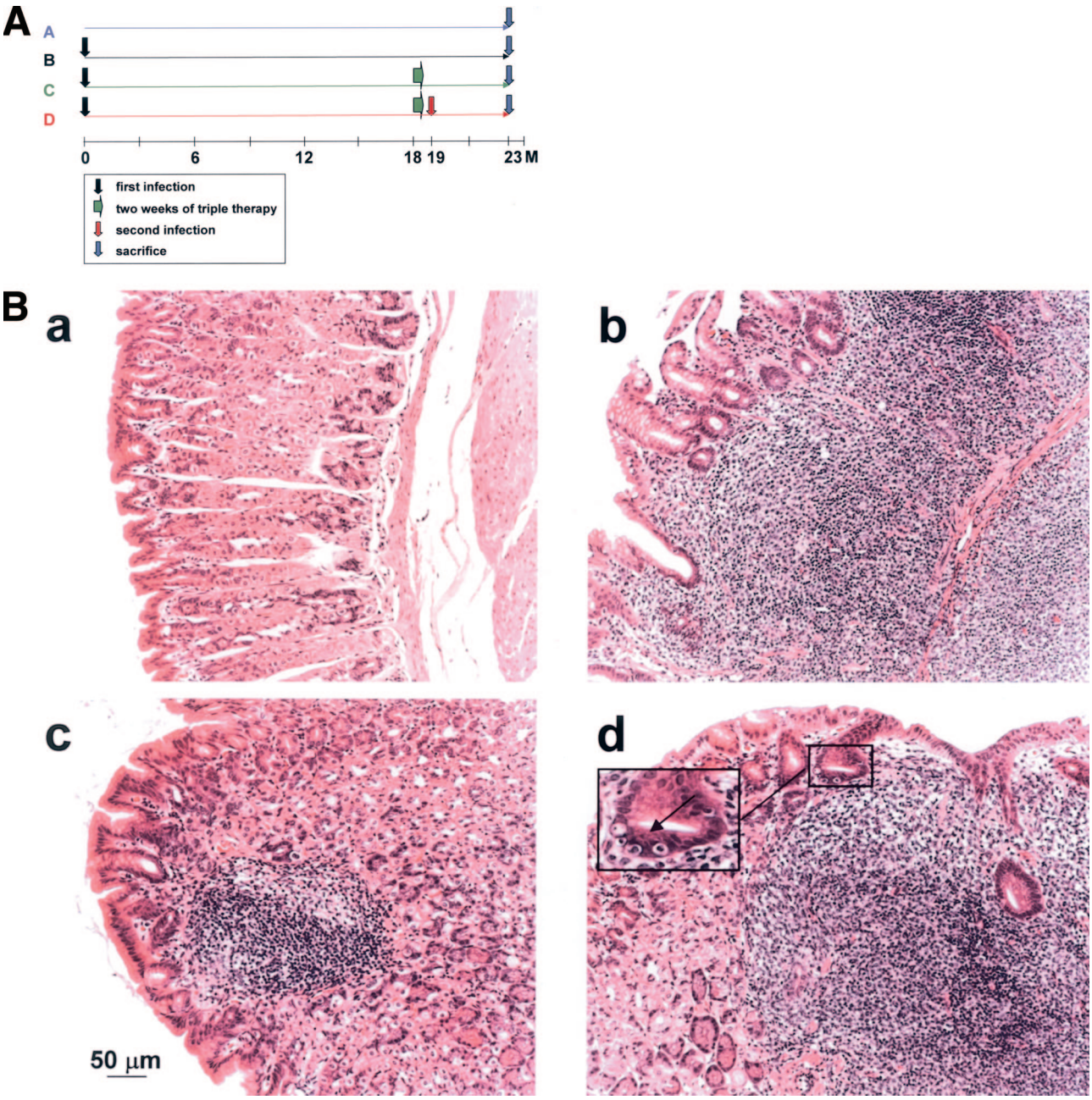

Figure 1. Effect of *Helicobacter* eradication therapy and re-infection on MALT lymphoma progression. Groups of 8 to 12 mice were either infected for 23 months with *Helicobacter felis* (group B); infected for 18 months and then treated with triple antibiotic therapy (group C); or infected for 18 months, treated, and then re-infected with the same strain (group D). An additional group was left untreated (group A). At 23 months after initial infection, all mice were sacrificed, their stomachs were removed, and the tissue was processed for histological analysis. **A:** Schematic showing the timeline of treatments of all four groups. **B:** Representative H&E-stained sections of a control animal (**a**) and animals of groups B, C and D (**b**, **c**, and **d**, respectively). Animals of groups B and D are characterized by massive lymphocytic infiltration and the destruction of the glandular architecture of the gastric body mucosa. The **arrow** in the **inset** in **d** points to a typical lympho-epithelial lesion, a gastric gland that has been invaded by multiple lymphocytes. Gastric sections of animals in group C closely resemble control sections; however, roughly one-half of all successfully treated animals in this group retain small mucosal lymphoid aggregates (**c**), which are not accompanied by destructive lympho-epithelial lesions. Two of eight animals in group C were resistant to eradication therapy; gastric sections from these mice resemble those of groups B and D (not shown).

mecula, CA), CD40 (1:25; polyclonal goat serum; Santa Cruz Biotech Inc., Santa Cruz, CA), CD28 (1:10; polyclonal goat serum; Santa Cruz Biotech Inc.), CD69 (1:10; Armenian hamster clone H1.2F3; Santa Cruz Biotech Inc.), and CD11c (1:50; Armenian hamster clone HL3; PharMingen/BD Biosciences). The detection was performed using biotinylated secondary antibodies in combination with horseradish-peroxidase-coupled streptavidin (Jackson ImmunoResearch, West Grove, PA) and the substrates DAB (Research Genetics/Invitrogen, Carlsbad, CA), Vector SG (silver-gray), or Vector NovaRed (Vector Labs, Burlingame, CA). All sections were counterstained with hematoxylin, methyl green, or nuclear fast red; dehydrated; and coverslipped with Permount (Fisher

Table 1. Evaluation of Colonization and Histopathology in the Four Treatment Groups

Group	Treatment	Colonization* (antrum)†	Lymphoid aggregates‡	Lymphoepithelial lesions‡	MALT lymphoma§
A	Nil	0	0	0	0/6
B	Hf alone	3.6	2.2	2.1	3/12
C1¶	Hf + TT	0	0.67	0.3	0/6
C2‖	Hf + TT	2.5	3.0	2.25	1/2
D	Hf + TT + Hf	3.3	2.3	2.1	4/9

*Paraffin sections were stained with May-Grünwald-Giemsa for grading of bacterial colonization on a 0 to 4-point scale in four different regions of the stomach (antrum, body, antrum/body, and body/cardia transitional zones).

†Colonization levels in the antrum are shown because they are representative of overall colonization.

‡Hematoxylin and eosin-stained sections were also evaluated for histopathological changes: the presence of lymphoid aggregates and lymphoepithelial lesions were graded on a 0 to 3 scale. All slides were coded and examined blind.

§A diagnosis of low-grade lymphoma was made independently (M.F.D.).

¶Six of eight animals in group C were successfully treated.

‖The treatment of two of eight animals in group C was not successful.

Hf, *Helicobacter felis*; TT, triple therapy.

Scientific, Pittsburgh, PA). A Zeiss Axiophot microscope equipped with an AxioCam digital camera and AXIOVISION 3.1. software (Zeiss) was used for documentation.

Results

Colonization Levels and Histopathology in Mice after Triple Therapy and Re-Infection

To assess the effect that eradication therapy and re-infection have on colonization densities and histopathology of BALB/c mice, 35 mice were divided into four groups (A-D; Figure 1A): 12 mice were infected for the duration of the experiment (23 months, "primarily infected group" B), 8 mice were infected together with group B but also received a 2-week triple therapy at 18 months after infection ("TT treated group" C), and 9 additional mice were infected and treated along with group C and subsequently re-infected 1 month after the start of triple therapy ("re-infected group" D). The final group of six mice received no treatment or infection ("control group" A). All mice were sacrificed at 23 months after initial infection; their stomachs were removed and analyzed histologically with respect to colonization densities and pathological changes.

The level and pattern of colonization seen in the animals in groups B and D were comparable with previous experiments.[22,23] The bacteria were found to preferentially colonize the antrum and to a lesser extent the body/cardia and antrum/body transitional zones as has been seen previously.[22] Six of the eight (75%) animals in group C were found to be successfully cleared of bacteria. This clearance rate was comparable with that obtained previously.[14] No bacteria were detected in the uninfected control group. Correspondingly, no inflammatory response indicative of MALT or MALT lymphoma was observed in the control animals (Figure 1B, a). In the six animals that were successfully cleared of *H. felis* infection ("group C1"), only small remnants or no MALT-type lymphoid aggregates were detected (Figure 1B, c). No lympho-epithelial lesions or frank lymphomas were diagnosed in any of these animals. In contrast, a moderate to severe cellular response, predominantly characterized by the presence of lymphoid aggregates and the formation of lympho-epithelial lesions, was observed in animals of groups B and D (Figure 1B, b and d, respectively), and in those animals in group C that resisted antimicrobial therapy ("group C2", not shown). Of all animals that proved to be colonized at the completion of the experiment, 35% were diagnosed with low-grade MALT lymphoma, as evidenced by the presence of centrocyte-like cells in the context of destructive lympho-epithelial lesions. Interestingly, the treatment groups differed in the proportion of animals with frank lymphomas: only 3 of 12 animals in group B were diagnosed with lymphoma (25%), whereas the number rose to 4 of 9 in group D (44%), indicating that the proportion of end-stage disease was higher upon re-infection (Table 1).

Transcriptional Profiling Reveals Gene Clusters Indicative of Infection Status and Pathology

Based on the apparent differences in pathology between the four treatment groups, we chose to analyze the transcriptional profiles of gastric tissues of all four treatment groups with the aim of identifying transcripts whose expression pattern correlates with treatment outcome. A representative subset of mice was selected for every group (total of 29); a heat diagram of the ~125 most highly de-regulated genes is shown in Figure 2. Several interesting conclusions could be drawn from this analysis. Most obviously, a pan B-cell signature was found in all stomachs that were infected with *H. felis* at some point in the animals' lives independent of the infection status at the time of harvest (groups B, C, and D; Figure 2). This signature is present also in the successfully eradicated mice of the triple-therapy-treated group. It is enriched for genes encoding the components of secretory IgA as well as CD40 and integrin β7, B-cell markers required for the interaction with activated T cells via CD40 ligand, and for the homing of B cells to mucosal surfaces of the gastrointestinal tract, respectively. The presence of this signature in gastric tissue samples can therefore be considered an excellent marker for past or present *Helicobacter* infection, even in the absence of histological evidence of bacteria or B cells.

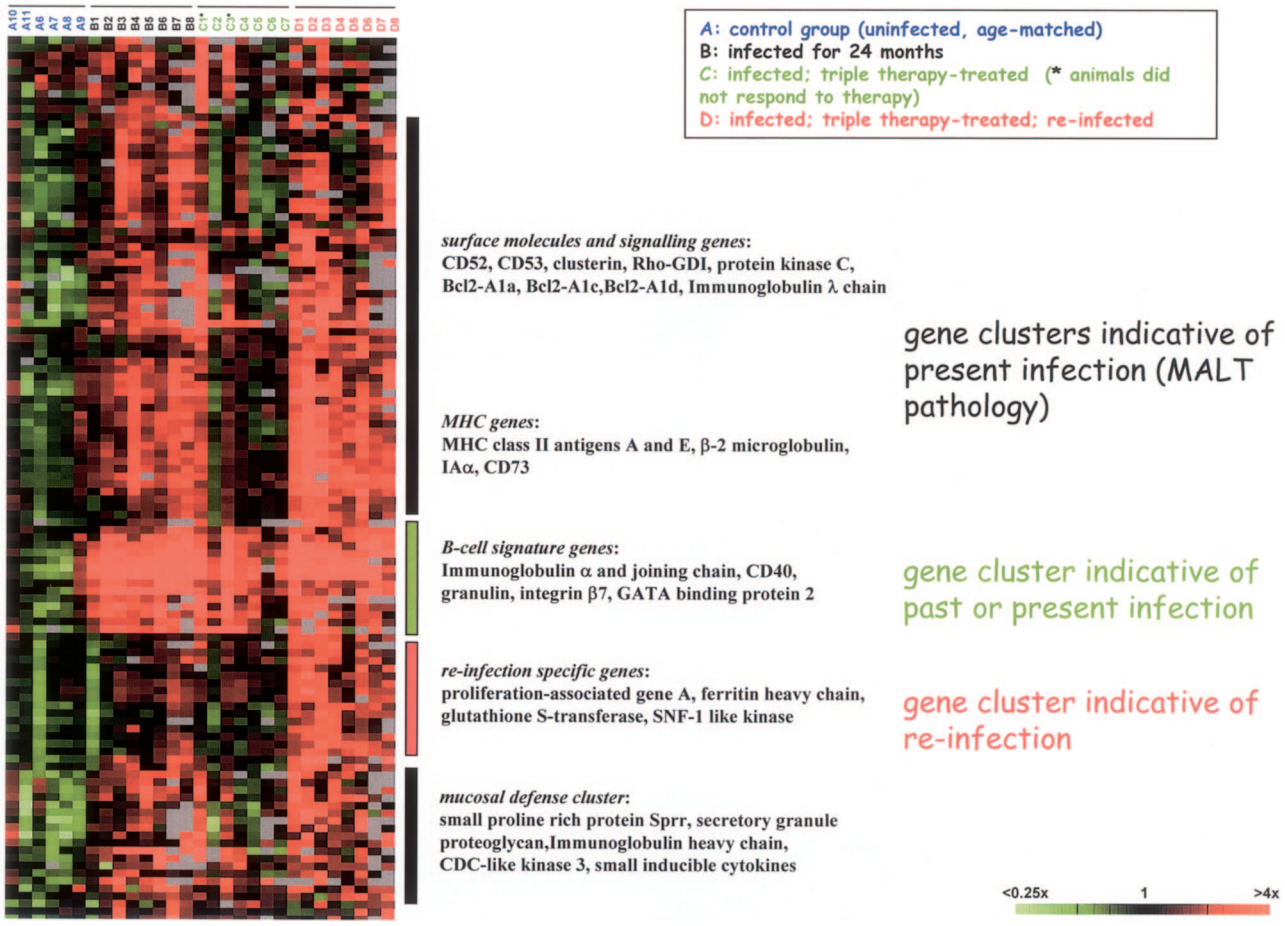

Figure 2. Transcriptional profiling reveals clusters of genes whose expression patterns correlate with treatment outcome. RNA was prepared from whole stomach tissue of several animals per treatment group, reverse transcribed, and hybridized to 38,000 element murine cDNA arrays. Data were filtered with respect to spot quality (spots with regression correlations <0.6 were omitted) and data distribution (genes whose $\log_2$ of red-to-green normalized ratio is more than 1.5 SD away from the mean in at least three arrays were selected) before clustering of the resulting 125 genes. Only genes for which information was available for >70% of arrays were included. Clusters of genes that are differentially regulated between treatment groups are annotated, and representative genes are listed for every cluster. The raw data for all of the arrays of this analysis are available at http://genome-www5.stanford.edu/.

A second cluster of genes is indicative of active *Helicobacter* infection at the time of harvest: it is uniformly present in all of the mice of groups B and D, as well as in those mice of group C that eluded eradication. This cluster is enriched for MHC genes (class I and II), as well as numerous cell surface receptors and signaling molecules, many of which are B cell specific (eg, other classes of immunoglobulin genes, CD52 and CD53, *Bcl*II-A1a, c, and d) and highly expressed in premalignant or malignant, but not normal, B cells. Of note in this cluster is one subset of genes that is not associated with lymphocytes, but rather reflects mucosal damage and/or a mucosal defense response. A marker typical of this subset is the small proline-rich protein, a factor that has been detected in numerous other screens for the effects of mucosal injury. The vast majority of genes in the "active infection" cluster has previously been described in our analysis of disease progression in the same model system and is discussed in detail elsewhere.[17]

Lastly and most unexpectedly, our transcriptional analysis uncovered a signature indicative of re-infection. All transcripts in this cluster are expressed at high levels in the animals that received triple therapy and were subsequently re-infected, but not at all or only at low levels in animals that were infected for the duration of the experiment. This cluster comprises genes encoding glutathione S-transferase and two kinases (deoxycytidine kinase and SNF1-like kinase) and most notably, the proliferation-associated gene A. Based on the intriguing finding that primarily infected and re-infected tissue profiles are similar but not identical and perhaps characterized by different rates of proliferation, we decided to pursue this lead further.

Lymphoid Aggregates in Primarily Infected, Successfully Treated, and Re-Infected Mice Differ with Respect to Proliferation Rates

To estimate the proliferative index of lymphoid aggregates found in the three relevant treatment groups, we stained paraffin sections from animals of groups B, C, and D with an antibody directed against proliferating cell nuclear antigen, a reliable nuclear marker of proliferation that works well on murine formalin-fixed, paraffin-embedded tissue samples (PCNA; Figure 3A, bottom panel). Adjacent sections were stained with hematoxylin and

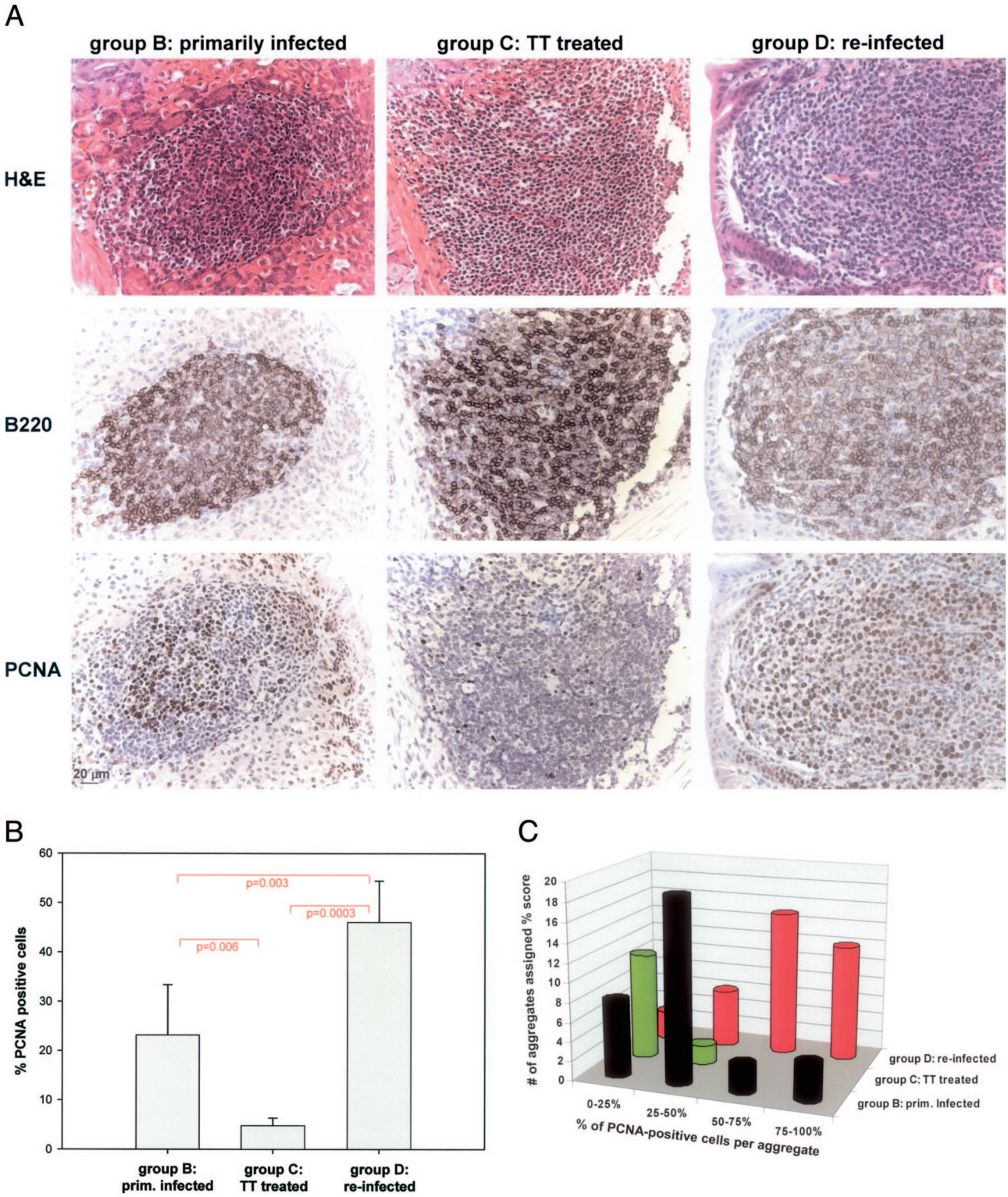

Figure 3. The proliferative index of lymphocytic aggregates correlates with treatment outcome. Serial paraffin sections of animals of groups B, C, and D were stained with antibodies against the B-cell marker B220, the proliferating cell nuclear antigen (PCNA), or H&E (as indicated on the **left** in **A**). **A:** Representative gastric sections from animals in groups B, C, and D. B220 immuno-reactivity is comparable in the three groups. In the case of PCNA, immuno-reactivity appears lowest in group C, intermediate in group B, and highest in group D. The immuno-reactivity of PCNA was evaluated quantitatively by two alternative approaches. **B:** PCNA-positive cells were counted in five or six representative aggregates per treatment group and the means (with error bars) are indicated as percentage of the total lymphocytic population. Pairs were subjected to an unpaired Student's *t*-test and the resulting *P* values are indicated. **C:** A total of 83 aggregates from all animals in the study were assigned one of four scores (0 to 25%, 25 to 50%, 50 to 75%, and 75 to 100%) indicative of PCNA reactivity. The number of aggregates assigned a certain score is indicated for every treatment group.

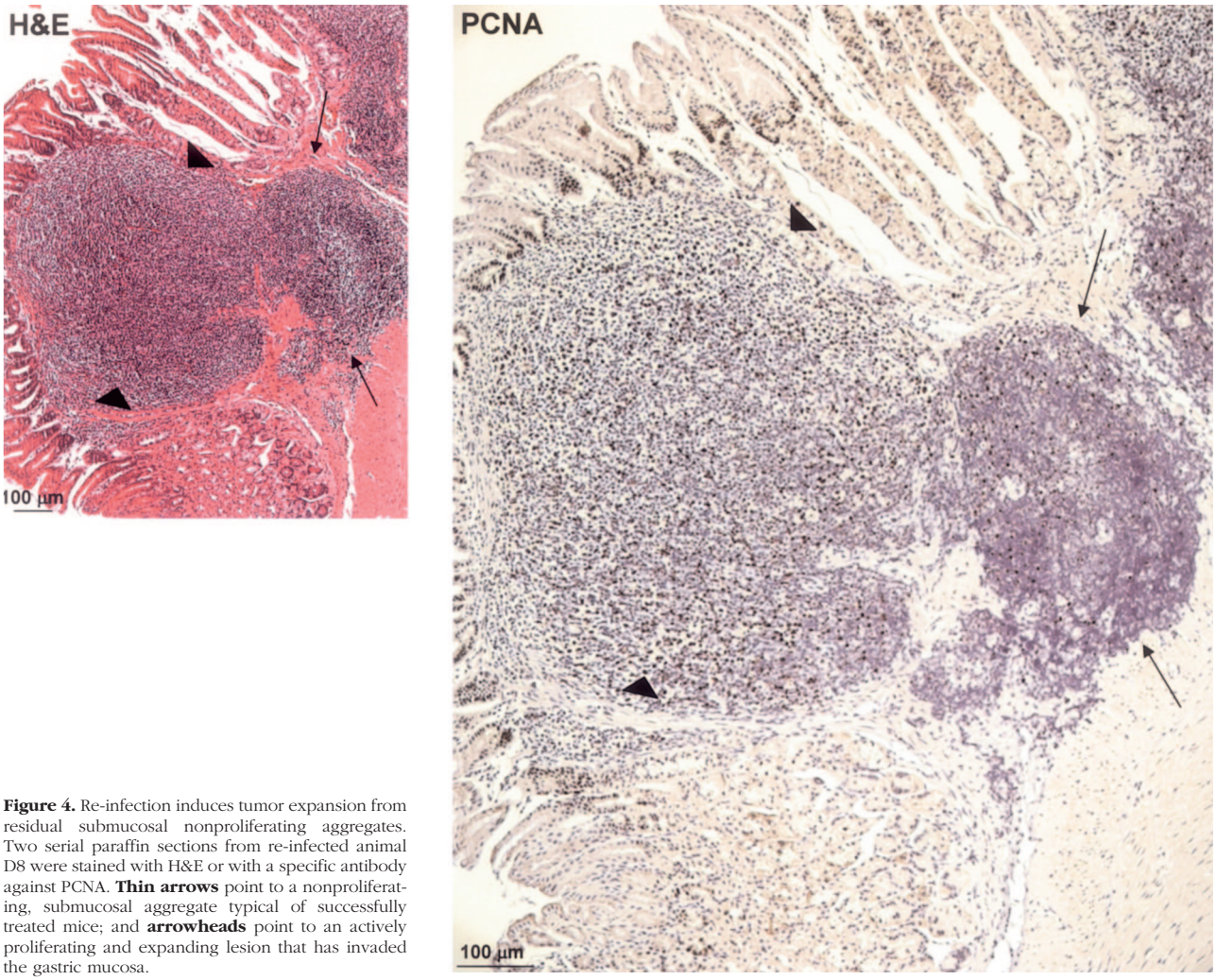

Figure 4. Re-infection induces tumor expansion from residual submucosal nonproliferating aggregates. Two serial paraffin sections from re-infected animal D8 were stained with H&E or with a specific antibody against PCNA. **Thin arrows** point to a nonproliferating, submucosal aggregate typical of successfully treated mice; and **arrowheads** point to an actively proliferating and expanding lesion that has invaded the gastric mucosa.

eosin or an antibody against the B-cell marker CD45R/B220 (Figure 3A, top and middle panels, respectively). The B220 panels reveal comparable staining patterns in all three groups, indicating that lymphoid aggregates consist in large part of B cells, independent of treatment. In contrast, the numbers of proliferating (PCNA-positive) cells vary dramatically between treatment groups (Figure 3A, bottom panel, and B and C). Whereas only between 3 and 7% of cells in lymphoid remnants of successfully eradicated mice stain positive for PCNA (mean of 4.8%, 6760 cells counted in six representative aggregates; Figure 3B), between 9 and 37% stain positive in primarily infected mice (mean of 23.2%, 9069 cells counted in six representative aggregates), and between 33 and 54% stain positive in re-infected mice (mean of 46%, 4732 cells counted in five representative aggregates; Figure 3B). The differences between all three pairs were statistically significant (Student's *t*-test; Figure 3B, *P* values). PCNA-positive cells were easily distinguished morphologically from noncycling cells by their large nuclei and extensive cytoplasm (Figure 3B, H&E-stained sections in top panel), features that give them a centrocyte-like appearance. Interestingly, the staining patterns of B220 and PCNA suggest that proliferating cells express lower levels of B220 on their surface than resting cells, indicating that B220 may be down-regulated during proliferation.

In addition to counting PCNA-positive cells and calculating the proliferative index of representative aggregates, we also quantified the proliferating population more broadly by evaluating the staining patterns of all lymphoid aggregates in two sections per mouse (83 aggregates total) and assigning them to one of four categories (0 to 25%, 25 to 50%, 50 to 75%, 75 to 100% positive cells). This analysis clearly confirmed the differences between the three treatment groups (Figure 3C). The results of both quantitative approaches taken together suggest that re-introduction of *H. felis* not only leads to very rapid tumor relapse in previously cured mice, but also gives rise to more aggressively cycling tumors.

Upon/After Re-Infection, Relapsing Tumors Expand from Clusters of Residual, Resting B Cells

During inspection of PCNA-stained sections of re-infected mice, we occasionally observed what appeared to

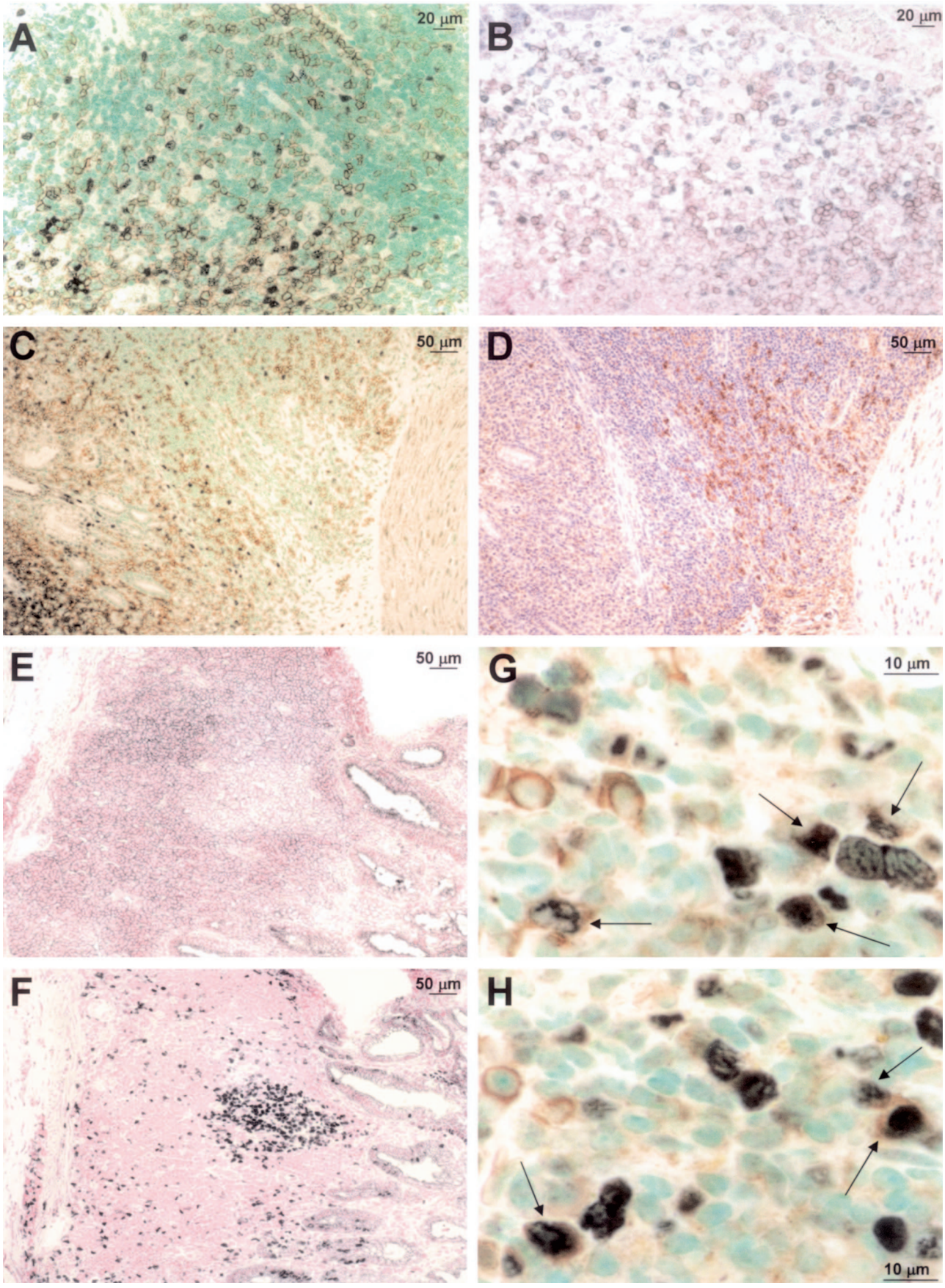
A
20 μm
B
20 μm
C
50 μm
D
50 μm
E
50 μm
G
10 μm
F
50 μm
H
10 μm

be the re-emergence of actively proliferating tumors from resting aggregates (Figure 4). In these areas, it seems as if clones of PCNA-positive tumor cells have invaded the mucosa from submucosal aggregates that strongly resemble the residual lymphoid remnants in triple-therapy-treated mice. These constellations were never seen in the other treatment groups. Based on this observation, we propose that the residual clusters of B cells found in the gastric mucosa of successfully eradicated mice can give rise to new lymphomas, which possibly explains the rapid course of tumor relapse in re-infected mice.

Proliferating Tumor Cells Are IgM^{high}, B220^{-}, CD40^{low}, CD79α^{-} B Cells

The surprising observation that CD45R/B220 appeared to be down-regulated in a proliferating subset of tumor cells prompted us to perform a more in-depth analysis of the immunophenotype of MALT lymphoma cells in our model system. Double labeling with PCNA-specific (blue-gray nuclei) and B220-specific antibodies (brown cell surface, Figure 5A) confirmed the virtually mutually exclusive staining pattern, raising the question of whether cycling tumor cells were in fact B cells at all. Double labeling of PCNA (blue-gray nuclei) and CD3 (brown cell surface) ruled out T cells, because these were also usually PCNA negative (Figure 5B). We then tested another pan-B-cell marker, CD79α, which associates noncovalently with surface Ig, forming the B-cell receptor. Surface expression of CD79α has been shown to begin at the pro-B-cell stage and persists throughout B-cell differentiation, but is down-regulated during B-cell activation and ceases completely around the onset of plasma cell differentiation. In our MALT lymphoma model, we detect groups of CD79α-positive cells (brown in Figure 5D), but these were consistently PCNA negative and B220 negative (Figure 5C). We next assayed for CD40, a constitutively expressed surface molecule that mediates the interaction of B cells with T cells through binding of CD40L (CD154). Although a large proportion of tumor cells in the lymphoid aggregates were strongly positive for CD40 (Figure 5E), the proliferating population (Ki67-positive, Figure 5F) was not (Figure 5, compare E and F): it expressed only low levels of CD40.

In contrast, many PCNA-positive cells expressed high levels of IgM on their surface (Figure 5, G and H, arrows), showing definitively that the actively proliferating tumor cells were B cells. MALT lymphoma cells in humans are also typically IgM^{+}, IgD^{-}, highlighting the similarities between both types of tumors. In conclusion, this phenotyping approach clearly demonstrated the enormous variability among MALT lymphoma cells, even those in one aggregate; multiple subsets of B cells with quite different properties could be distinguished in the same lesion.

Tumor-Infiltrating T Cells Are Predominantly CD4^{+} and of the Type 2 Helper T-Cell (Th2) Type

Previous studies have shown that tumor-infiltrating T cells mediate the response of tumor B cells to *Helicobacter* antigen: in human MALT lymphoma biopsy samples cultured *in vitro*, death of the tumor cells can be prevented by addition of heat inactivated *H. pylori*, and this effect is abrogated by depletion of T cells from the culture.[24] Our own results indicate that large numbers of T cells also infiltrate low-grade lymphomas of mice (Figure 5B).[16] We were therefore interested in learning more about the types of T cells involved in this response. Figure 6 shows a representative lymphoid aggregate stained with antibodies against markers that distinguish subsets of T cells. Although the majority of cells in the aggregate are clearly non-proliferating B cells (B220-positive), T cells are ubiquitous as evidenced by CD3 staining (Figure 6). Macrophages are found only around the edges of the tumor and are present at very low numbers (F4/80 panel). Of the CD3-positive T cells, the majority are CD4-positive, indicating a large T-helper subpopulation. However, a significant CD8-positive population is also found in the aggregate (Figure 6). We estimate the CD4:CD8 ratio to be approximately 4:1.

Helper T cells can be categorized into T-helper (Th) 1 and 2 subsets that have very different functions. Each subtype is defined and characterized by the secretion of specific sets of cytokines. A Th1 cell typically produces large amounts of interferon (IFN)-γ, IL-2, and tumor necrosis factor-α, whereas a Th2 cell predominantly releases IL-4, -5, -9, -10, and -13. We used specific immunohistochemical staining for IFN-γ and IL-4 to discriminate between the subsets in our model system: interestingly, we found very little IFN-γ but strong IL-4 reactivity, indicating that the majority of CD4-positive cells infiltrating low-grade lymphomas are of the Th2 type (Figure 6).

Dendritic Cells Are the Predominant Antigen-Presenting Cell Type in MALT Lymphoma

T cells need to express costimulatory receptors in order to become optimally activated upon antigen recognition. One such receptor is CD28, which binds to the B7-related surface protein CD80 (B7.1) on antigen-presenting cells. We tested for CD28 expression on tumor-infiltrating T cells by immunohistochemistry and detected high levels of CD28 on their surface, indicating that these cells are immunocompetent (Figure 7). We further tested

Figure 5. Immunophenotype of proliferating lymphoma cells. Paraffin or cryosections were stained with the following antibodies: **A**, B220 (brown surface signal) and PCNA (blue-gray nuclear signal) with methyl green counterstaining; **B**, CD3 (brown surface signal) and PCNA (blue-gray nuclear signal) with nuclear fast red counterstaining; **C**, B220 (brown surface signal) and PCNA (blue-gray nuclear signal) with methyl green counterstaining; **D**, CD79 (brown surface signal) with hematoxylin counterstaining—**C** and **D** are serial sections; **E**, CD40 (blue-gray surface signal) with nuclear fast red counterstaining; **F**, Ki67 (blue-gray nuclear signal) with nuclear fast red counterstaining—**E** and **F** are serial sections; **G** and **H**, IgM (brown surface signal) and PCNA (blue-gray nuclear signal) with methyl green counterstaining. **Arrows** indicate double labeling with both antibodies. Scale bars are included in every micrograph.

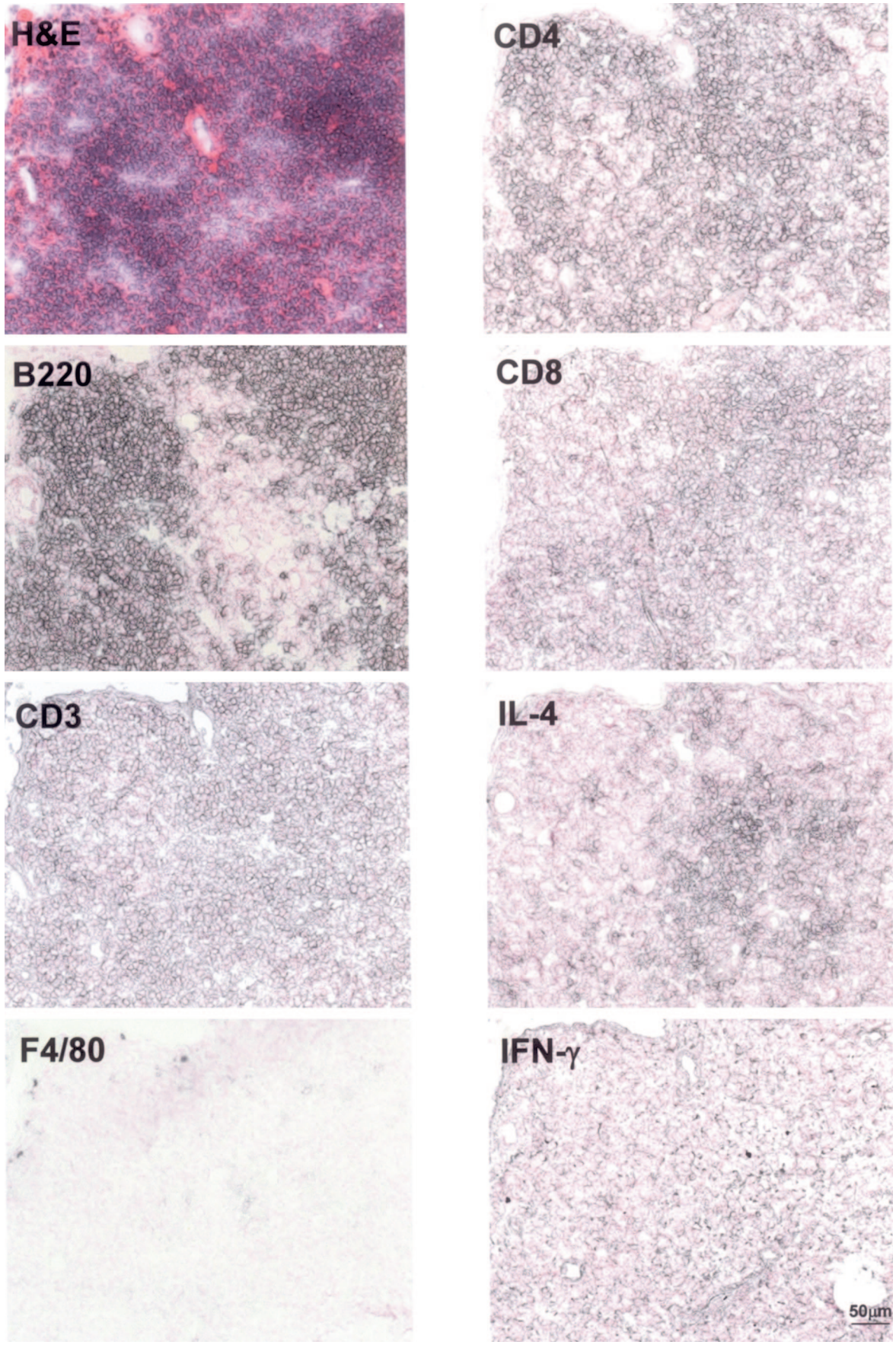
H&E
CD4
B220
CD8
CD3
IL-4
F4/80
IFN-γ
50μm

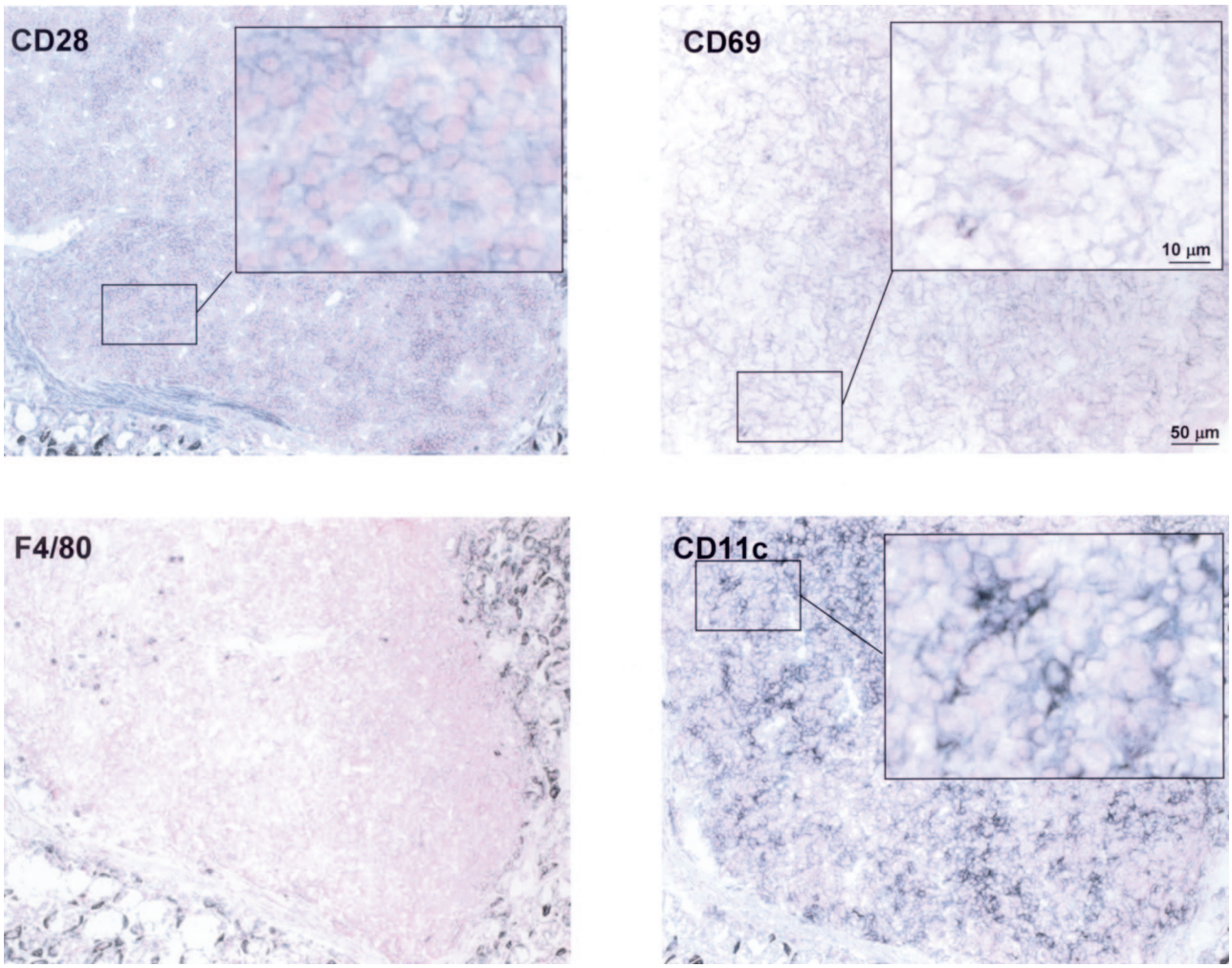

Figure 7. Tumor-infiltrating T cells are activated and immunocompetent, and dendritic cells constitute the predominant antigen-presenting cell type in MALT lymphoma. Serial cryosections were stained with antibodies against the indicated antigens and counterstained with nuclear fast red. CD28 is a costimulatory receptor of T cells, and CD69 is a T-cell activation marker. CD11c is a pan-dendritic cell marker, and F4/80 is a macrophage marker. Areas of interest are shown at high magnification. Scale bars representative of all panels are included in the top right micrographs.

whether tumor-infiltrating T cells are activated; surface expression of CD69, which is among the earliest antigens to appear after activation of T cells, indicated T-cell activation in the environment of MALT tumors (Figure 7).

Numerous reports suggest that MALT lymphomas express antigen receptors with specificity for autoantigens;[25–27] therefore, the tumor B cells are unlikely to play a role in the presentation of *Helicobacter* antigen to tumor-infiltrating T cells. We hypothesized that either macrophages or dendritic cells should fulfill this function. As indicated above, we found MALT lymphomas to be surprisingly devoid of macrophages; only very few F4/80-positive cells can be detected in the periphery of the tumor, and this cell type seems to be virtually excluded from the tumor mass (Figures 6 and 7). In contrast, large numbers of CD11c-positive dendritic cells populate the tumors, suggesting that they are the main source of antigen presentation to intratumoral T cells (Figure 7). Further subclassification using antibodies against markers of myeloid, lymphoid, and follicular dendritic cell populations (CD11b, CD8α, and S100, respectively) indicate that the majority of resident dendritic cells fall into the latter category, whereas myeloid and lymphoid dendritic cells are not found (data not shown; Figure 8).

The Numbers of Tumor-Infiltrating Dendritic Cells Correlate with Severity of Disease

MALT lymphoma B cells depend on the stimulation by *Helicobacter*-specific accessory cells; based on our findings, we believe those are follicular dendritic as well as Th2-polarized $CD4^+$ T cells. We therefore asked whether the numbers of tumor-infiltrating accessory cells corre-

Figure 6. Phenotypic characterization of tumor-infiltrating immune cells. Serial cryosections were stained in blue-gray with monoclonal antibodies against the indicated antigens and counterstained with nuclear fast red. An H&E-stained section is included for orientation. Lymphoid aggregates are colonized by $CD3^+$ T cells, but not $F4/80^+$ macrophages. $B220^+$ B cells constitute the predominant cell type. Tumor-infiltrating T cells are mostly $CD4^+$ and produce IL-4, but not IFN-γ. A scale bar is included in the bottom right panel.

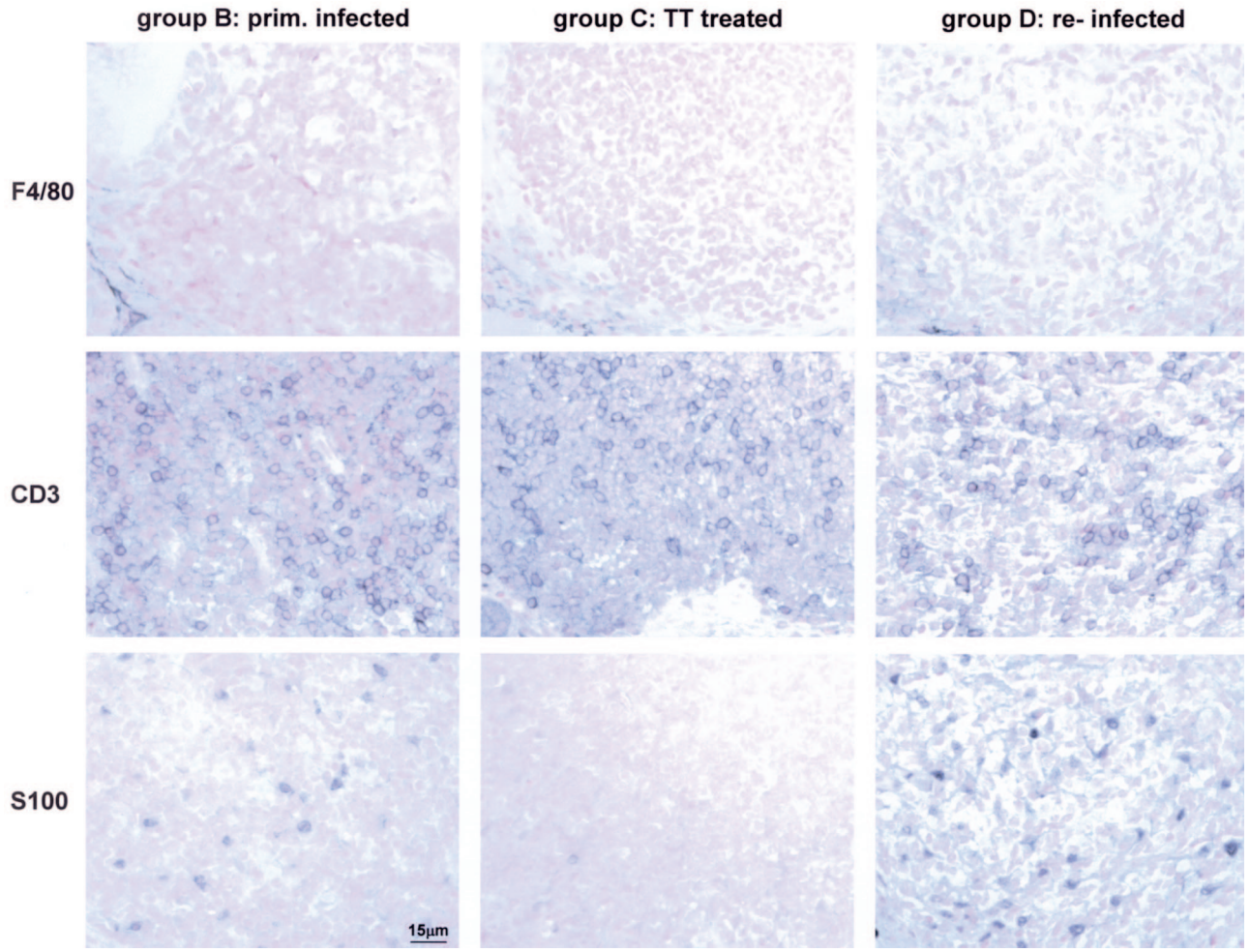

Figure 8. Numbers of tumor-infiltrating follicular dendritic cells but not T cells or macrophages correlate with and are indicative of treatment outcome. Serial paraffin sections of animals of groups B, C, and D were stained with antibodies against the macrophage marker F4/80, the T-cell marker CD3, and the follicular dendritic cell marker S100 and counterstained with nuclear fast red. A scale bar representative of all panels is included in the bottom left micrograph.

lated with experimental treatment, disease outcome, or the percentage of cycling cells in the tumor mass. Interestingly, the density and distribution of CD3-positive T cells was identical in lymphoid aggregates of primary and relapsed tumors and even in the residual aggregates typical of regressed tumors (Figure 8, middle panels).

F4/80-positive macrophages were confined to the edges of lymphoid aggregates in all three treatment groups, consistent with their proposed irrelevance in MALT lymphoma pathogenesis (Figure 8, top panels). As with T cells, the numbers of macrophages did not change in response to *Helicobacter* elimination or re-infection. In contrast, when inspecting the staining pattern of the follicular dendritic cell marker S100, we detected major differences between treatment groups. Whereas $S100^{+}$ dendritic cells were rarely observed in lymphoid remnants characteristic of successfully treated mice, the numbers were considerably higher in lesions induced by primary infection and highest in lesions induced by re-infection (ie, primary tumors and relapsed tumors, Figure 8, bottom panels). The distribution of dendritic cells was also quite distinct: they are typically most highly concentrated in areas of the tumor facing the glandular epithelium and the gastric lumen where they are most likely to encounter *Helicobacter* (Figure 8, right panel in bottom row).

Our findings suggest that although lesion-infiltrating T cells likely play a role in triggering the proliferation of B cells in lymphoid aggregates, their overall numbers do not correlate with and are probably not a good indicator of tumor behavior. In contrast, high numbers and a characteristic distribution of follicular dendritic cells in close proximity to the gastric lumen are typical of aggressive, actively cycling tumors.

Discussion

Persistent infection of BALB/c mice with several *Helicobacter* species results in the development of gastric low-grade MALT lymphoma with features that are strikingly similar to the human form of the malignancy: late onset of disease, propensity to high-grade transformation, occasional spreading to lymph nodes and spleen, and dependence on active infection with *Helicobacter*. In humans as well as mice, the disease is treatable in the majority of

cases by eradication of the bacterium, a unique feature of this type of tumor.[11,14] However, the long-term stability of complete remission is unclear, and recent evidence suggests that eradication therapy may be less efficient than combined radiochemotherapy in achieving long-term, sustained remission.[28] Despite the great clinical relevance of this issue, the precise trigger of tumor relapse, and, more specifically, the role that *Helicobacter* (re-)infection may play in the recurrence of MALT lymphomas, has to date not been addressed in depth. Our mouse model of the disease allows convenient manipulations of infection status such as antibiotic eradication therapy and re-infection and therefore is well suited to address these questions experimentally. We have used the model system to determine 1) how eradication therapy affects progression of the lymphoma, 2) whether disease relapse occurs on re-introduction of *Helicobacter*, and 3) whether the course of the disease is different in relapsed compared with primary lesions. Several conclusions could be drawn from the study.

Eradication Therapy Leads to Clearance of Bacteria and Complete Histopathological, but Not Molecular Remission

Of the mice that received triple therapy, 75% were cleared of the infection, and their histopathological lesions regressed. This is in agreement with treatment outcomes in patients, where remission rates between 50 and 83% are typically achieved.[11,29–33] Failure of patients to respond to eradication therapy has recently been attributed to a chromosomal translocation at t(11;18)(q21;21), resulting in the API2-MALT1 fusion transcript;[34] in contrast, the same translocation is not predictive of a negative response to chemotherapy.[35] We are currently investigating the prevalence of this chromosomal abnormality and its potential effect on treatment outcome in the murine system.

The stomachs of mice that responded favorably to treatment were either entirely devoid of MALT or retained very minor residual noninvasive lymphoid aggregates at 5 months after treatment (the end point of the study). However, transcriptional profiling of whole stomach tissues from these mice consistently revealed the persistence of B cells in all successfully treated, ie, *Helicobacter*-free, mice. These cells shared some of the molecular features of active MALT lymphomas, such as high levels of transcripts encoding secretory IgA and a number of B-cell surface markers, but lacked others such as high levels of MHC class I and II, CD52, and Bcl-2. A similar phenomenon has been observed in patients, where persistence of monoclonal immunoglobulin heavy chain sequences in the gastric mucosa of roughly 50% of patients with complete histological remission has been documented.[32,36] Therefore, it has to be assumed that complete histological remission after eradication therapy is not equivalent to "molecular" remission, implying that frequent and long-term follow-up of patients is indicated. The relatively high risk of relapse after eradication therapy as opposed to chemotherapy can possibly be attributed to the gastric persistence of residual, resting lymphocytes.

Re-Infection Induces Rapid Disease Recurrence and Relapsed Tumors Are More Aggressive Than Primary Tumors

Re-introduction of the original strain after eradication therapy led to recurrence of destructive lympho-epithelial lesions in 100% of mice. This finding is quite remarkable because it suggests that immunity against *Helicobacter* is not acquired even after life-long infection, despite a vigorous and sustained immune response. In keeping with our result, the natural re-infection rate in the human adult population has been proposed to be just as high or only slightly lower than the primary infection rate.[37] Because both the infection and the re-infection rates in adults are low (estimated at 1 to 2% in the general population), recurrence of tumors due to re-infection is relatively uncommon, affecting anywhere from 1.1 to 20% of successfully treated patients (1 in 7 patients[38]; 1 in 90[33]; 3 in 15[39]; 2 in 17[40]; case reports in[41,42]). In fact, disease recurrence in humans is more likely to be due to failure of the primary eradication than to new infection.[37] Nevertheless, in light of the finding that 97% of spouses of patients with *H. pylori*-positive low-grade MALT lymphomas are also sero-positive (far exceeding the seroprevalence rates in the general population,[43]), it has been suggested that spouses receive eradication therapy along with patients to eliminate this common source of re-infection.[43]

In contrast to the primary premalignant and malignant lesions, which take between 15 and 18 months to develop in the BALB/c model, relapsed lesions were observed only 4 months after re-infection, indicating that the course of relapse is extremely rapid. This is reflected by highly reproducible differences in the transcriptional profiles and higher proliferative indices in the relapsing compared with the primary lesions. Moreover, a higher proportion of mice in the re-infected group than in the primarily infected group displayed frank low-grade lymphomas as opposed to premalignant lesions, perhaps indicating that the disease is aggravated by eradication and subsequent re-infection. Similar observations have been reported sporadically for MALT lymphoma patients. Two case reports in particular describe the rapid recurrence of MALT lymphomas in patients, both of which were attributed to re-infection rather than recrudescence.[41,42] In these cases, the tumors had re-emerged 3 and 6 months after a follow-up examination confirmed complete histological remission.[41,42] In the discussion of the clinical course of disease in these cases, the authors speculated that *H. pylori* eradication in MALT lymphoma patients may lead to persistence of the neoplasia in a "latent form" and "subsequently, re-exposure to the bacterium might determine prompt reactivation of the neoplastic cells, already sensitized to the *H. pylori* antigen stimulus, with a spectacularly rapid expansion of the neoplasia."[42] This is particularly remarkable because

gastric low-grade lymphoma is generally accepted to be an indolent, slowly progressing malignancy.

The Role of Accessory Cells in MALT Lymphoma Pathogenesis

The proliferation of MALT lymphoma cells in the early stages of the disease is not autonomous but depends on direct and/or indirect signals provided by *Helicobacter*-specific tumor-infiltrating T cells. In the absence of T cells, explanted tumor B cells cannot be rescued from apoptosis or induced to proliferate by addition of heat-inactivated *H. pylori*.[24] We performed a detailed immunohistochemical analysis to characterize accessory cell populations *in vivo*. Our data strongly suggest that the majority of tumor-infiltrating T cells is $CD4^+$, with an estimated ratio of $CD4^+/CD8^+$ cells of approximately 4:1. Roughly 30% of $CD4^+$ cells produce IL-4, a typical Th2 cytokine, whereas expression of the Th1 cytokine IFN-γ was not detected. Our result is in line with the *in vitro* findings of Greiner et al,[44] who cultured explanted MALT lymphoma cells of six patients in the CD40 system, ie, under continued anti-CD40 activation. In this system, addition of IL-4, but not IFN-γ or IL-2 ,synergized with CD40 ligation to trigger lymphoma B-cell proliferation. These authors further reported high levels of Th2 and Th3 but not Th1 cytokine transcripts in MALT lymphoma biopsies as measured by reverse transcription PCR.[45]

IL-4 induces proliferation of B cells that have been activated through their B-cell receptor. Th2 cells are essential for efficient mucosal antibody responses, which apparently are mounted by the lymphoma cells as evidenced by our detection of high levels of IgA-specific transcripts *in vivo*. MALT lymphoma B cells are believed to retain many features of normal B cells[44] and should therefore be able to respond to IL-4. Taking these considerations into account, it seems conceivable that the paracrine signals provided by tumor-infiltrating *H. pylori*-reactive Th2 cells could be of decisive importance for the pathogenesis of MALT lymphoma, especially in the early stages of lymphomagenesis when the tumors are still antigen-dependent. In contrast, the local cytokine response in *H. pylori* infected duodenal ulcer and gastritis patients is of the Th1 type;[46,47] in fact, chronic gastritis is now widely accepted to be a Th1 driven disease, with IFN-γ being the main cytokine responsible for gastritis-associated pathology.[48,49]

This apparent dichotomy in *H. pylori* infected patients, some of whom are more prone to Th1-mediated diseases whereas others develop Th2-mediated diseases, is mirrored by the BALB/c-C57BL6 dichotomy in experimentally infected mice. BALB/c mice, which are genetically prone to high production of Th2 cytokines and the associated B-cell response, develop MALT lymphoma, but do not show symptoms of gastritis or ulcers.[13] C57BL6 mice, in contrast, mount a predominantly Th1-polarized response against *H. pylori* and do not develop MALT lymphoma, but are prone to chronic gastritis, which can progress to gastric adenocarcinoma via the precursor lesions atrophic gastritis, intestinal metaplasia, and dysplasia.[49–51] Elucidation of the genetic basis for the dramatic differences between the two mouse strains should also be useful in explaining and predicting disease outcomes in infected human populations.

In vitro and molecular studies suggest that MALT lymphoma B cells are antigen-sensitive, but autoreactive.[27,52,53] Therefore, we hypothesized that other antigen-presenting cells should be involved in activating the effector mechanisms of tumor-infiltrating T-helper cells. We found that a third major cellular component of MALT lymphomas besides B and $CD4^+$ T cells are $CD11c^+$ dendritic cells, which make up one-fifth to one-third of the tumor mass. They express neither myeloid nor lymphoid markers, indicating that they belong to neither of these defined dendritic cell subpopulations. Rather, we find that a subset expresses the follicular dendritic cell marker S100. Moreover, the number of tumor-infiltrating follicular dendritic cells is clearly correlated with disease outcome. Tumor regression in response to eradication therapy leads to an almost complete disappearance of dendritic cells from residual clusters of B cells, probably reflecting the elimination of *Helicobacter* from these mice. In contrast, follicular dendritic cells populate primary MALT lymphomas, and, to an even greater extent, tumors that have relapsed because of re-infection. Interestingly, our gene expression data confirm this result, because many of the genes involved in antigen presentation ("gene clusters indicative of past or present infection") follow a very specific expression pattern across arrays (Figure 2). They are not at all expressed in tissues from successfully treated mice but show intermediate expression levels in primary tumors and high expression in relapsed tumors.

Interestingly, the results of our previous study on the molecular progression of MALT lymphoma in the mouse model[17] are confirmed by the data reported here. In that study, we identified a marker, Calgranulin A, which faithfully distinguishes premalignant from malignant lesions in the murine system. Calgranulin is synonymous for S100, and the Calgranulin A protein is detected by the S100-specific antibody we used in this study to stain follicular dendritic cells. Only malignant tumors (the primary and relapsed tumors in our current study), but not premalignant or regressed lesions, are infiltrated by large numbers of dendritic cells, which are reflected in the expression profiles by elevated levels of their marker gene, Calgranulin A. The results of both our tumor progression and regression studies taken together imply that the dendritic cell may be an important new target in MALT lymphoma therapy.

Acknowledgments

We thank the members of the Falkow/Tompkins and Amieva laboratories for helpful discussions and Ronald Levy, Lucy Thompson, and Trevor Lawley for critical comments on the manuscript.

References

1. Isaacson PG, Du MQ: MALT lymphoma: from morphology to molecules. Nat Rev Cancer 2004, 4:644–653
2. Du MQ, Isaccson PG: Gastric MALT lymphoma: from aetiology to treatment. Lancet Oncol 2002, 3:97–104
3. Wyatt JI, Rathbone BJ: Immune response of the gastric mucosa to Campylobacter pylori. Scand J Gastroenterol 1988, 142 (Suppl.):44–49
4. Stolte M, Eidt S: Lymphoid follicles in antral mucosa: immune response to Campylobacter pylori? J Clin Pathol 1989, 42:1269–1271
5. Isaacson PG: Gastric MALT lymphoma: from concept to cure. Ann Oncol 1999, 10:637–645
6. Genta RM, Hamner HW, Graham DY: Gastric lymphoid follicles in Helicobacter pylori infection: frequency, distribution, and response to triple therapy. Hum Pathol 1993, 24:577–583
7. Nakamura S, Yao T, Aoyagi K, Iida M, Fujishima M, Tsuneyoshi M: Helicobacter pylori and primary gastric lymphoma: a histopathologic and immunohistochemical analysis of 237 patients. Cancer 1997, 79:3–11
8. Eidt S, Stolte M, Fischer R: Helicobacter pylori gastritis and primary gastric non-Hodgkin's lymphomas. J Clin Pathol 1994, 47:436–439
9. Wotherspoon AC, Ortiz-Hidalgo C, Falzon MR, Isaacson PG: Helicobacter pylori-associated gastritis and primary B-cell gastric lymphoma. Lancet 1991, 338:1175–1176
10. Parsonnet J, Hansen S, Rodriguez L, Gelb AB, Warnke RA, Jellum E, Orentreich N, Vogelman JH, Friedman GD: Helicobacter pylori infection and gastric lymphoma. N Engl J Med 1994, 330:1267–1271
11. Wotherspoon AC, Doglioni C, Diss TC, Pan L, Moschini A, de Boni M, Isaacson PG: Regression of primary low-grade B-cell gastric lymphoma of mucosa-associated lymphoid tissue type after eradication of Helicobacter pylori. Lancet 1993, 342:575–577
12. Wotherspoon AC: Gastric lymphoma of mucosa-associated lymphoid tissue and Helicobacter pylori. Annu Rev Med 1998, 49:289–299
13. Enno A, O'Rourke JL, Howlett CR, Jack A, Dixon MF, Lee A: MALToma-like lesions in the murine gastric mucosa after long-term infection with Helicobacter felis: a mouse model of Helicobacter pylori-induced gastric lymphoma. Am J Pathol 1995, 147:217–222
14. Enno A, O'Rourke J, Braye S, Howlett R, Lee A: Antigen-dependent progression of mucosa-associated lymphoid tissue (MALT)-type lymphoma in the stomach: effects of antimicrobial therapy on gastric MALT lymphoma in mice. Am J Pathol 1998, 152:1625–1632
15. Sutton P, O'Rourke J, Wilson J, Dixon MF, Lee A: Immunisation against Helicobacter felis infection protects against the development of gastric MALT Lymphoma. Vaccine 2004, 22:2541–2546
16. Mueller A, O'Rourke J, Chu P, Kim CC, Sutton P, Lee A, Falkow S: Protective immunity against Helicobacter is characterized by a unique transcriptional signature. Proc Natl Acad Sci USA 2003, 100:12289–12294
17. Mueller A, O'Rourke J, Grimm J, Guillemin K, Dixon MF, Lee A, Falkow S: Distinct gene expression profiles characterize the histopathological stages of disease in Helicobacter-induced mucosa-associated lymphoid tissue lymphoma. Proc Natl Acad Sci USA 2003, 100:1292–1297
18. Dick-Hegedus E, Lee A: Use of a mouse model to examine anti-Helicobacter pylori agents. Scand J Gastroenterol 1991, 26:909–915
19. van Zanten SJ, Kolesnikow T, Leung V, O'Rourke JL, Lee A: Gastric transitional zones, areas where Helicobacter treatment fails: results of a treatment trial using the Sydney strain mouse model. Antimicrob Agents Chemother 2003, 47:2249–2255
20. Sherlock G, Hernandez-Boussard T, Kasarskis A, Binkley G, Matese JC, Dwight SS, Kaloper M, Weng S, Jin H, Ball CA, Eisen MB, Spellman PT, Brown PO, Botstein D, Cherry JM: The Stanford Microarray Database. Nucleic Acids Res 2001, 29:152–155
21. Eisen MB, Spellman PT, Brown PO, Botstein D: Cluster analysis and display of genome-wide expression patterns. Proc Natl Acad Sci USA 1998, 95:14863–14868
22. Danon SJ, O'Rourke JL, Moss ND, Lee A: The importance of local acid production in the distribution of Helicobacter felis in the mouse stomach. Gastroenterology 1995, 108:1386–1395
23. Lee A, Chen M, Coltro N, O'Rourke J, Hazell S, Hu P, Li Y: Long term infection of the gastric mucosa with Helicobacter species does induce atrophic gastritis in an animal model of Helicobacter pylori infection. Zentralbl Bakteriol 1993, 280:38–50
24. Hussell T, Isaacson PG, Crabtree JE, Spencer J: Helicobacter pylori-specific tumour-infiltrating T cells provide contact dependent help for the growth of malignant B cells in low-grade gastric lymphoma of mucosa-associated lymphoid tissue. J Pathol 1996, 178:122–127
25. Qin Y, Greiner A, Trunk MJ, Schmausser B, Ott MM, Muller-Hermelink HK: Somatic hypermutation in low-grade mucosa-associated lymphoid tissue-type B-cell lymphoma. Blood 1995, 86:3528–3534
26. Greiner A, Marx A, Heesemann J, Leebmann J, Schmausser B, Muller-Hermelink HK: Idiotype identity in a MALT-type lymphoma and B cells in Helicobacter pylori associated chronic gastritis. Lab Invest 1994, 70:572–578
27. Hussell T, Isaacson PG, Crabtree JE, Spencer J: The response of cells from low-grade B-cell gastric lymphomas of mucosa-associated lymphoid tissue to Helicobacter pylori. Lancet 1993, 342:571–574
28. Alpen B, Kuse R, Parwaresch R, Muller-Hermelink HK, Stolte M, Neubauer A: Ongoing monoclonal B-cell proliferation is not common in gastric B-cell lymphoma after combined radiochemotherapy. J Clin Oncol 2004, 22:3039–3045
29. Montalban C, Manzanal A, Boixeda D, Redondo C, Bellas C: Treatment of low-grade gastric MALT lymphoma with Helicobacter pylori eradication. Lancet 1995, 345:798–799
30. Stolte M, Eidt S: Healing gastric MALT lymphomas by eradicating H pylori? Lancet 1993, 342:568
31. Roggero E, Zucca E, Pinotti G, Pascarella A, Capella C, Savio A, Pedrinis E, Paterlini A, Venco A, Cavalli F: Eradication of Helicobacter pylori infection in primary low-grade gastric lymphoma of mucosa-associated lymphoid tissue. Ann Intern Med 1995, 122:767–769
32. Bertoni F, Conconi A, Capella C, Motta T, Giardini R, Ponzoni M, Pedrinis E, Novero D, Rinaldi P, Cazzaniga G, Biondi A, Wotherspoon A, Hancock BW, Smith P, Souhami R, Cotter FE, Cavalli F, Zucca E: Molecular follow-up in gastric mucosa-associated lymphoid tissue lymphomas: early analysis of the LY03 cooperative trial. Blood 2002, 99:2541–2544
33. Fischbach W, Goebeler-Kolve ME, Dragosics B, Greiner A, Stolte M: Long term outcome of patients with gastric marginal zone B cell lymphoma of mucosa associated lymphoid tissue (MALT) following exclusive Helicobacter pylori eradication therapy: experience from a large prospective series. Gut 2004, 53:34–37
34. Liu H, Ye H, Ruskone-Fourmestraux A, De Jong D, Pileri S, Thiede C, Lavergne A, Boot H, Caletti G, Wundisch T, Molina T, Taal BG, Elena S, Thomas T, Zinzani PL, Neubauer A, Stolte M, Hamoudi RA, Dogan A, Isaacson PG, Du MQ: T(11;18) is a marker for all stage gastric MALT lymphomas that will not respond to H. pylori eradication. Gastroenterology 2002, 122:1286–1294
35. Streubel B, Ye H, Du MQ, Isaacson PG, Chott A, Raderer M: Translocation t(11;18)(q21;q21) is not predictive of response to chemotherapy with 2CdA in patients with gastric MALT lymphoma. Oncology 2004, 66:476–480
36. Thiede C, Wundisch T, Alpen B, Neubauer B, Morgner A, Schmitz M, Ehninger G, Stolte M, Bayerdorffer E, Neubauer A: Long-term persistence of monoclonal B cells after cure of Helicobacter pylori infection and complete histologic remission in gastric mucosa-associated lymphoid tissue B-cell lymphoma. J Clin Oncol 2001, 19:1600–1609
37. Parsonnet J: What is the Helicobacter pylori global reinfection rate? Can J Gastroenterol 2003, 17 (Suppl. B):46B–48B
38. Papa A, Cammarota G, Tursi A, Gasbarrini A, Gasbarrini G: Helicobacter pylori eradication and remission of low-grade gastric mucosa-associated lymphoid tissue lymphoma: a long-term follow-up study. J Clin Gastroenterol 2000, 31:169–171
39. Tursi A, Cammarota G, Papa A, Cuoco L, Fedeli G, Gasbarrini G: Long-term follow-up of disappearance of gastric mucosa-associated lymphoid tissue after anti-Helicobacter pylori therapy. Am J Gastroenterol 1997, 92:1849–1852
40. Nobre-Leitao C, Lage P, Cravo M, Cabecadas J, Chaves P, Alberto-Santos A, Correia J, Soares J, Costa-Mira F: Treatment of gastric MALT lymphoma by Helicobacter pylori eradication: a study controlled by endoscopic ultrasonography. Am J Gastroenterol 1998, 93:732–736
41. Horstmann M, Erttmann R, Winkler K: Relapse of MALT lymphoma associated with Helicobacter pylori after antibiotic treatment. Lancet 1994, 343:1098–1099
42. Cammarota G, Montalto M, Tursi A, Vecchio FM, Fedeli G, Gasbarrini G: Helicobacter pylori reinfection and rapid relapse of low-grade B-cell gastric lymphoma. Lancet 1995, 345:192

43. Fischbach W, Jung T, Goebeler-Kolve M, Eck M: Comparative analysis of the Helicobacter pylori status in patients with gastric MALT-type lymphoma and their respective spouses. Z Gastroenterol 2000, 38:627–630
44. Greiner A, Knorr C, Qin Y, Sebald W, Schimpl A, Banchereau J, Muller-Hermelink HK: Low-grade B cell lymphomas of mucosa-associated lymphoid tissue (MALT-type) require CD40-mediated signaling and Th2-type cytokines for in vitro growth and differentiation. Am J Pathol 1997, 150:1583–1593
45. Knorr C, Amrehn C, Seeberger H, Rosenwald A, Stilgenbauer S, Ott G, Muller Hermelink HK, Greiner A: Expression of costimulatory molecules in low-grade mucosa-associated lymphoid tissue-type lymphomas in vivo. Am J Pathol 1999, 155:2019–2027
46. Lindholm C, Quiding-Jarbrink M, Lonroth H, Hamlet A, Svennerholm AM: Local cytokine response in Helicobacter pylori-infected subjects. Infect Immun 1998, 66:5964–5971
47. Ahlstedt I, Lindholm C, Lonroth H, Hamlet A, Svennerholm AM, Quiding-Jarbrink M: Role of local cytokines in increased gastric expression of the secretory component in Helicobacter pylori infection. Infect Immun 1999, 67:4921–4925
48. Lohoff M, Rollinghoff M, Sommer F: Helicobacter pylori gastritis: a Th1 mediated disease? J Biotechnol 2000, 83:33–36
49. Smythies LE, Waites KB, Lindsey JR, Harris PR, Ghiara P, Smith PD: Helicobacter pylori-induced mucosal inflammation is Th1 mediated and exacerbated in IL-4, but not IFN-gamma, gene-deficient mice. J Immunol 2000, 165:1022–1029
50. Wang TC, Dangler CA, Chen D, Goldenring JR, Koh T, Raychowdhury R, Coffey RJ, Ito S, Varro A, Dockray GJ, Fox JG: Synergistic interaction between hypergastrinemia and Helicobacter infection in a mouse model of gastric cancer. Gastroenterology 2000, 118:36–47
51. Sakagami T, Dixon M, O'Rourke J, Howlett R, Alderuccio F, Vella J, Shimoyama T, Lee A: Atrophic gastric changes in both Helicobacter felis and Helicobacter pylori infected mice are host dependent and separate from antral gastritis. Gut 1996, 39:639–648
52. Qin Y, Greiner A, Hallas C, Haedicke W, Muller-Hermelink HK: Intraclonal offspring expansion of gastric low-grade MALT-type lymphoma: evidence for the role of antigen-driven high-affinity mutation in lymphomagenesis. Lab Invest 1997, 76:477–485
53. Greiner A, Knorr C, Qin Y, Schultz A, Marx A, Kroczek RA, Muller-Hermelink HK: CD40 ligand and autoantigen are involved in the pathogenesis of low-grade B-cell lymphomas of mucosa-associated lymphoid tissue. Dev Immunol 1998, 6:187–195